Research papers

Sediment fate and transport: Influence of sediment source and rainfall

Sanghyun Lee, Maria L. Chu [*], Jorge A. Guzman

Department of Agricultural and Biological Engineering, University of Illinois at Urbana-Champaign, Urbana, IL, USA

ARTICLE INFO

ABSTRACT

The capability of hydrologic models to spatially simulate the changes in hydrologic processes, like precipitation, is an important consideration in capturing the impacts of these processes on sediment prediction across the domain. Radar-derived precipitation (RDP) provides an enhanced detail of rainfall characteristics in time and space compared to estimates from rain-gauge precipitation (RGP) commonly used in hydrologic modeling. However, the impacts of these datasets on sediment fate and transport depend on how sediment sources were conceptualized in the model. This paper developed a modeling framework to simulate sediment transport from upland to the stream and to the outlet of the watershed based on a gridded conceptualization and to examine the impacts of RGP and RDP with different types of sediment sources on sediment prediction. The Water Erosion Prediction Project (WEPP) model was used to estimate daily sediment sources in a semi-distributed and fully distributed manner using the hydrologic model, MIKE SHE and MIKE 11. Model comparison was performed in a watershed in Illinois characterized by a dominant agricultural landscape. The results indicated that the use of RDP only ensured better model performance for sediment yield with the fully distributed sediment source. That is, combining both the ability of the RDP to capture the spatial variability of rainfall across the watershed and assessing sediment production at higher resolution improved the accuracy of predictions in sediment yield while decreasing uncertainties associated with sediment simulations. Advancing modeling capabilities will require the development of new modeling platforms that aim to seamlessly integrate large-scale distributed simulations and environmental input data at finer spatial resolutions.

1. Introduction

It is widely known that the integration of the spatio-temporal characteristics of precipitation in distributed hydrologic models is fundamental to advance the predictions of flow and transport phenomena at a watershed scale. Rainfall is a crucial variable in hydrologic modeling, and its misrepresentation in time and space may result in the inaccurate convolution of subsequent processes related to water quantity and quality (Chaplot et al., 2005; Wei et al., 2009). As an example, sediment load and its associated transport of organic and inorganic compounds are source-dependent (Syvitski et al., 2000), highlighting the importance of the distributed simulation of the major drivers controlling soil erosion. In particular, detailed rainfall characteristics across a watershed may help improve the capacity of hydrologic models to represent better sediment sources, surface routing, and the expected suspended load in streams (Chaplot et al., 2005; Usón and Ramos, 2001). However, the capability of hydrologic models to spatially simulate the changes in hydrologic processes, like precipitation, is an important consideration in

capturing the impacts of these changes on sediment prediction across the domain. Above all, simulating sediment production and transport using distributed models to fully capture precipitation's spatial variability is crucial in developing a holistic sediment prediction scheme.

It is apparent that the spatial variability of precipitation and sediment production poses a challenge in predicting sediment transport due in part to the uncertainties brought by how these two processes are represented in space and their complex interactions. There have been previous research efforts to improve sediment predictions from lumped or semi-distributed models using spatially varied precipitation. As an example, radar-derived precipitation (RDP) has been used in predicting soil loss using either the Universal Soil Loss Equation (USLE; Wischmeier and Smith, 1978) or the Water Erosion Prediction Project (WEPP) model (Flanagan and Nearing, 1995). Fischer et al. (2018) utilized RDP in the USLE model to minimize the error arising from input data. However, the disagreements from the prediction were still observed due mainly to parameterization in that the parameters such as management factors do not reflect inter-annual variations. To reflect realistic field conditions,

RDP and remotely sensed parameters were used in predicting soil loss using the Water Erosion Prediction Project (WEPP) model (Gelder et al., 2018). However, soil loss in this study was reported only as average annual hillslope erosion or sediment yield (sheet/rill), not including ephemeral gully soil erosion at a sub-catchment scale (90 km^2) and sediment transport between the sub-catchments was not considered and thus the validation of the model could not be provided. In addition, to capture the spatial variability of rainfall, RDP had been used to estimate areal precipitation in the semi-distributed models (e.g. SWAT model) for predicting sediment yield (Di Luzio and Arnold, 2004; Gao et al., 2017; Kalin and Hantush, 2006). However, the impacts of the use of RDP in semi-distributed models for sediment predictions were not discussed. To better represent the spatial distribution of eroded soil and its transport, soil erosion should be evaluated at a finer scale that can reflect fine resolution input data used in the model. That is, the use of RDP does not guarantee a better sediment prediction if the soil loss was predicted at a coarser level. However, none of the current studies evaluated the impacts of the use of RDP on sediment prediction in fully distributed settings.

In this study, we hypothesized that distributed precipitation will improve sediment prediction only if sediment sources are spatially distributed. Specifically, we explored the following hypotheses, to examine the impacts of distributed and semi-distributed sediment sources on sediment predictions under RDP and rain-gauge precipitation (RGP):

1. The improved streamflow predictions that stemmed directly from RDP would improve sediment transport and yield predictions.
2. The spatial variations in precipitation would improve sediment transport predictions regardless of streamflow predictions.
3. The use of RDP would improve sediment predictions only where sediment sources are spatially distributed.

We developed four models to simulate sediment transport from upland to the stream and to the outlet of the watershed using gauged and radar precipitation in combination with a gridded conceptualization (distributed) and sub-catchments level discretization (semi-distributed) sediment sources. The simulation results based on these four models were compared and examined to test each hypothesis.

2. Methodology

2.1. Model description

The study area is an intensively-managed agricultural watershed in central Illinois, with an area of approximately 660 km^2 (Fig. 1). The watershed is located in a temperate climate zone, receiving a total annual average rainfall of 1,000 mm (IEPA, 2007). The topography of the watershed is relatively flat, with an average slope of 1%, and most of the land is used for row crops (90%). In this watershed, the four separate models were developed for continuous, multiannual simulations in an agricultural watershed to incorporate the three hypotheses. To determine whether hypotheses 1 and 2 are acceptable, the RDP and RGP were separately assigned as Radar and Gauge (Table 1). The RDP was assigned based on the National Weather Service/National Centers for Environmental Prediction stage IV QPE (Lin, 2011), while the RGP was simulated based entirely on precipitation from rain gauges (Rantoul and Normal) using Thiessen polygon (Fig. 1a). Note that the NCEP stage IV product is a CONUS QPE 4 km grid precipitation collected from the National Oceanic and Atmospheric Administration (NOAA) River Forecast Centers. To determine whether hypothesis 3 is valid, the sediment source across the watershed was estimated using the WEPP model and the semi-distributed and distributed sediment sources were estimated at sub-catchment and grid levels, respectively. The watershed was discretized into 300-m grid cells and 49 sub-catchments (Fig. 1b) in the distributed and semi-distributed models, respectively, for sediment sources (Table 1). To simulate the fate and transport of sediment across

Table 1
Different types of inputs used in four separate models.

Model ID	Sediment source	Precipitation
D-R	Distributed	Radar
D-G	Distributed	Gauge
S-R	Semi-distributed	Radar
S-G	Semi-distributed	Gauge

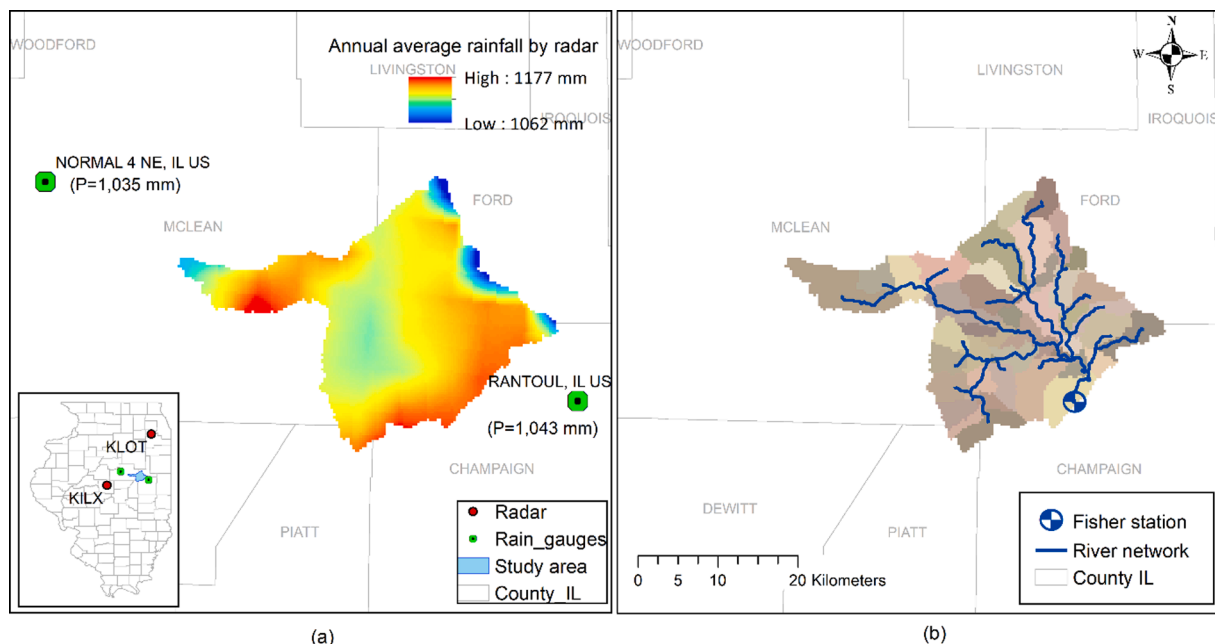(a)   (b)

Fig. 1. Study area with (a) the spatial distribution of average total annual precipitation estimates by radar from 2013 to 2019 across the watershed including radar sites (KILX and KLOT) and (b) 49 sub-catchments used for semi-distributed sediment source prediction (for model ID: S-R and S-G). P values near the rain gauges indicate average total annual precipitation estimated by point observations from 2013 to 2019.

the watershed, the fully distributed hydrologic model, MIKE-SHE, coupled with the one-dimensional hydrodynamic river model, MIKE 11 (Refsgaard and Storm, 1995) was used.

2.1.1. Precipitation impacts

To determine whether or not spatially varied precipitation can improve sediment predictions (hypothesis 1 and 2), two sets of precipitation data were used to quantify the differences of simulation results in streamflow and sediment discharges. The hydrologic models commonly represent precipitation as time-dependent areal variables in which precipitation is linked to the nearest station-based observation. This variable is commonly interpolated from neighboring stations, statistically estimated using intensity–durationfrequency curves, or defined as an areal partition using Thiessen polygons, also known as the Dirichlet/Voronoi polygons. The use of areal precipitation estimates may result in the misrepresentation of sediment prediction on a mesoscale analysis (hr-day, and 2–2000 km distance; Orlanski, 1975) due to the coarse granularity of available gauge networks (Pathak and Teegavarapu, 2018).

RDP provides an enhanced detail of rainfall characteristics across space compared to observations from RGP commonly used in hydrologic modeling. However, rainfall estimates based on stand-alone radar systems are subject to several potential issues such as radar beam blockage (Nelson et al., 2010), bright band enhancement (Smith et al., 1996), anomalous propagation (Krajewski and Vignal, 2001), and uncertainty of microphysical parameters of Z-R relationships (Smith et al., 1996; Vasiloff et al., 2007). To provide better precipitation estimates, multiple sensors such as radars and rain gauges were fused to quantitatively enhance precipitation estimates (QPE) across the mesoscale (Pathak and Teegavarapu, 2018).

To assess hypotheses 1 and 2, two sets of daily precipitation inputs were created, one was based on the multi-sensor QPE (NCEP stage IV analysis), and the other was based entirely on ground-based observations, the closest to the watershed being the Normal and Rantoul stations (Fig. 1a). The spatial discretization of the modeled processes across the watershed was set to 300×300 m, for a total of 7,303 grid cells. To assign distributed precipitation at each grid cell, the stage IV data were linearly resampled to 300 m (hereafter, called radar). In contrast, the gauged precipitation was determined using the Thiessen polygon method and then resampled to a 300 m spatial resolution (hereafter, called gauge). Note that the Thiessen polygon is a common practice in hydrologic modeling where ground-based observations are used to represent the homogenous precipitation across large areas.

The spatial variation of the averaged total annual precipitation (2013–2019) estimated by radar ranged from 1,062 mm $year^{-1}$ to 1,177 mm $year^{-1}$ (Fig. 1a). In contrast, precipitation at the Rantoul and Normal weather stations (gauged precipitation) was 1,043 mm $year^{-1}$ and 1,035 mm $year^{-1}$, respectively. The radar was on average higher for the watershed than the gauge over seven years resulting in an annual total average of 1,138 mm $year^{-1}$ and 1,038 mm $year^{-1}$ for radar and gauge, respectively.

A point-pair comparison of the radar- and gauge-based precipitation was conducted by comparing the rainfall observations at Rantoul and Normal stations (Fig. 1a) and the radar estimates in their nearest-neighboring grid cells, where the rain gauges were located. This was performed to determine how the two types of precipitation varied in terms of annual precipitation total, monthly precipitation average, and rain-day frequency from 2013 to 2019. For the rain-day frequency analysis, the daily precipitation<0.1 mm was assumed as a non-rainy day, and the rain-day was classified for light precipitation ($0.1 \leq P < 4$ mm day^{-1}), moderate precipitation ($4 \leq P < 20$ mm day^{-1}), and heavy precipitation ($P \geq 20$ mm day^{-1}) (Arnone et al., 2013). Daily precipitation for each class was randomly sampled with replacement using bootstrapping to calculate the average rain-day frequency for each class with 95% confidence intervals.

2.1.2. Sediment source impacts

To examine hypothesis 3, whether or not the semi- and distributed sediment sources would impact the sediment predictions, the WEPP model (Flanagan and Nearing, 1995) was used to provide the sediment source in two different modes, semi-distributed and distributed modes. The WEPP model is a continuous, process-based model that predicts soil loss and sediment deposition along hillslopes, as well as in small agricultural watersheds. In this study, we utilized only the hillslope erosion component of WEPP. It simulates sheet and rill erosion at a field scale based on the raindrop impacts, surface runoff generation, hydraulic shear stress, and sediment load in the flow. The model was known to be applicable to a broad range of soil and climate conditions (Laflen et al., 2004; Tiwari et al., 2000; Zhang et al., 1996).

For distributed sediment sources, the watershed was discretized into 300-m grid cells for a total of 7,303 cells across the watershed. Each grid cell was conceptualized as a single hillslope with a unique combination of climate, topography, soil, and land use. Thus, the time series of sediment sources in each grid have different values of sediment production throughout the watershed. On the other hand, for semi-distributed sediment sources, the watershed was divided into 49 sub-catchments (Fig. 1b), and each grid in one sub-catchment is assumed to have the same properties of slope, soil, land use. The average slope was used for each sub-catchment and dominant soil properties and land use were extracted from a corresponding sub-catchment. Therefore, 49 WEPP simulations were performed for all sub-catchments at the same scale as in the distributed model, and assigned the equivalent time series within each sub-catchment. For precipitation inputs, observed precipitation were used depending on the types of precipitation inputs (Table 1) for the simulation period. The land uses were determined from the National Agricultural Statistics Service (NASS) (USDA, 2016), and the following management practices were considered for the analysis based on survey data conducted by Illinois Department of Agriculture (IDOA, 2018): (1) no-till (2) mulch-till (3) reduced-till and (4) conventional tillage. A more detailed description of land use and tillage systems for this watershed can be found in the paper of Lee et al. (2021).

For both inputs, the simulation results of sediment leaving the hillslope predicted from the WEPP model were inserted as sediment sources in the distributed hydrologic model to transport the eroded soil across the watershed.

2.1.3. Water movement

The hydrologic processes across the watershed and in the river were simulated by a physically-based distributed model, MIKE SHE and a 1D hydrodynamic model MIKE 11, respectively. The MIKE SHE model simulated the overland, unsaturated, and saturated flows while MIKE 11 simulated the propagation of the hydrograph once the water reaches the river. The hydrologic components in the coupled model included 1-D Richard equation for the unsaturated flow; Kristensen and Jensen method (1975) for the actual evapotranspiration; 2-D diffusive wave approximation for the overland flow; 1-D Saint Venant equations for the main channel and kinematic wave approximation for upstream tributaries; and 3-D Darcy's law for the saturated flow. A detailed description of the MIKE SHE model can be found in Refsgaard and Storm (1995). The parameters of MIKE SHE, being a physically-based model, are measurable in the field and thus input data were directly extracted from observation data. The average slope of the watershed was approximately 1% obtained from the 30 m digital elevation model (DEM) (USGS, 2016). The soil properties were extracted from the Soil Survey Geographic Database (SSURGO) (USDA, 2017), and the land cover information was obtained from the Cropland Data Layer (CDL) (USDA, 2016), mostly occupied by corn (48%) and soybeans (40%). However, due to the spatial variability of some parameters that were not adequately sampled, calibration was performed to properly account for these variabilities. Subsurface drainage through tile drains was conceptualized by a linear reservoir model, as a function of a drain level and a time constant, and these two parameters were calibrated by comparing

streamflow discharge at Fisher station (Fig. 1b) (Botero-Acosta et al., 2019).

2.1.4. Sediment movement

The MIKE SHE and MIKE 11 models were used to transport sediment from the surface to the river network, and to the outlet of the watershed through the rivers. The fate and transport of sediment in the watershed were simulated by 1-D and 2-D advection–dispersion equations (ADE) with sink and source terms for sediment transport in rivers and overland flow, respectively, assuming the suspended sediment is completely mixed over the depth of water. In the overland flow, sediment production for each grid estimated by the WEPP model was added as a source term in the ADE, while the rate of deposition (S_d) and erosion (S_e) as sink and source terms in the ADE in the rivers can be expressed by

$$S_d = \frac{wc}{h^*}\left(1 - \frac{\tau}{\tau_{cr}}\right) \ for \ \tau < \tau_{cr} \tag{1}$$

where c is the sediment concentration, w is the mean fall velocity of suspended particles, h^* is the mean depth that the particles settle, τ is shear stress of bed and τ_{cr} is the critical shear stress. Deposition along the stream occurs when τ is less than τ_{cr}.

$$S_e = \frac{M^*}{h}\left(\frac{\tau}{\tau_{cr}} - 1\right)^b \ for \ \tau \geq \tau_{cr} \tag{2}$$

where M^* is the erodibility of the bed, h is the flow depth, and b is the erosion exponent. Erosion along the river only occurs when τ is greater than or equal to τ_{cr}. Note that the erosion rate is affected by the local hydraulic conditions, and the deposition rate is affected by both local hydraulic conditions and sediment concentration.

2.2. Model performance

Four combinations of precipitation and sediment source data were used to simulate the streamflow and sediment load at the outlet of the watershed. The Fisher station (Fig. 1b), located at the outlet of the watershed was used as an assessment endpoint of the combinations of input datasets. To evaluate the performance of the models in simulating streamflow and sediment, the Nash-Sutcliffe efficiency (NSE) (Nash and Sutcliffe, 1970), the mean absolute difference (MAD), and root-mean-square error (RMSE) between simulations (s) and observations (o) were used (Eqs. (3)–(5)). Note that the NSE ranges from $-\infty$ to 1 where NSE equal to 1 means a perfect match between the simulated and observed variables, while MAD and RMSE decrease with increasing model accuracy.

$$NSE = 1 - \frac{\sum (s_i - o_i)^2}{\sum (o_i - \bar{o})^2} \tag{3}$$

$$MAD = \frac{\sum |s_i - o_i|}{n} \tag{4}$$

$$RMSE = \sqrt{\frac{\sum (s_i - o_i)^2}{n}} \tag{5}$$

2.3. Sediment rating curve

Due to the lack of continuous sediment data within the simulation period, a sediment rating curve was used to estimate the sediment discharge as the power-law equation (Azadi et al., 2020; Syvitski et al., 2000; Tfwala and Wang, 2016).

$$Q_s = a Q_w^b \tag{6}$$

where Q_s is the suspended load, Q_w is the flow discharge, and a and b are the sediment rating coefficient and exponent, respectively. The 153

sediment grab samples collected from the Fisher station from 1979 to 1997 were used to derive the rating curve. Considering that the main source of sediment in this watershed is from agricultural production (Rhoads et al., 2016), the total number of samples was divided into the growing season (May-October) and non-growing season (November-April) groups (Fig. 2). These two groups showed distinguishable patterns in terms of sediment load at low to moderate flow, generating higher sediment load in the growing season than in the non-growing season. To apply the rating curves to the simulation period, it was assumed that the relationship between sediment and streamflow discharge remains constant over time. This assumption was based on the channelization at a large portion of the streams, and no significant changes in land use since the 1940 s, mostly occupied by agriculture (Rhoads et al., 2016; Urban and Rhoads, 2003). In addition, the two years of survey data (2017–2018) conducted by the Illinois Department of Agriculture (IDOA, 2018) showed that conventional tillage is still dominantly used and the rate of conservation practices such as no-till is low in this watershed. Therefore, it was inferred that changes in management practices were also not significant. Furthermore, the watershed response to rainfall was examined based on the annual runoff coefficient using the rainfall at Rantoul station and streamflow discharge at Fisher station from 1979 to 2019. The Spearman's rank correlation coefficient (r) indicated that there were no significant changes in the watershed response to rainfall over the period of record ($r = 0.18$). With this assumption, the two sediment rating curves were separately applied to estimate the daily sediment load for the growing and non-growing seasons based on the observed streamflow discharge for the simulation periods. Hereafter, the predicted sediment discharge based on the sediment rating curve was called observed sediment. Note that streambank erosion is an important driver in sediment transport that must be included in future research aimed at including unaccounted processes to advance model prediction.

3. Results and discussion

3.1. Model calibration

The calibration was performed in a previous study (Lee et al., 2021) that the hydrologic model was set-up and tested in two periods (1995–1999 and 2009–2013) and showed good agreements with the measured data, with NSE values of 0.57 and 0.50, respectively (Fig. 3a and 3b). Since WEPP and MIKE SHE/MIKE 11 models are physically-based models with inputs and parameters that are directly measurable
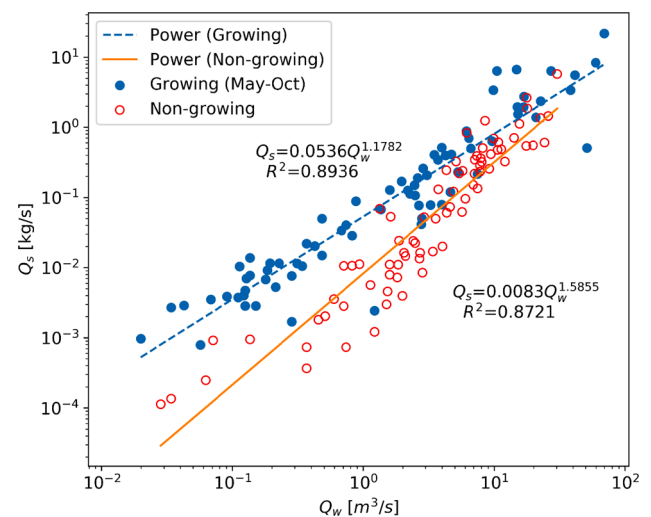

Fig. 2. Scatter plot of streamflow discharge (Q_w) and sediment discharge (Q_s) for the growing season (May-October) and non-growing season (November-April). The lines represent sediment rating curves for each group.
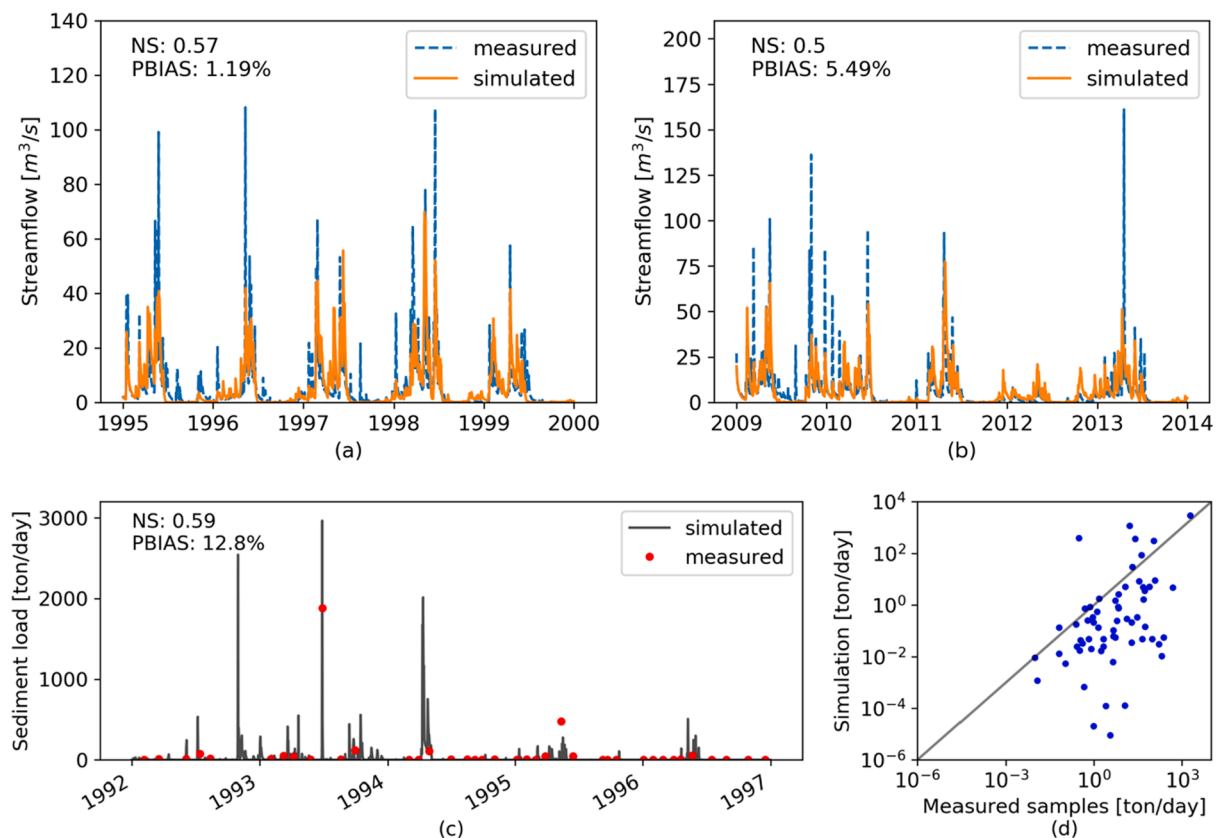
Fig. 3. Streamflow comparisons for (a) first period (1995–1999) and (b) second period (2009–2013), and (c) sediment load comparison from 1992 to 1996 and (d) scatter plot for simulation results and observations for sediment with 1:1 line at Fisher station (Lee et al., 2021).

from the field, no calibration is supposed to be needed. However, effective hydraulic conductivities in WEPP model and measurements of the parameters of the sink and source terms in the ADE (Table 2) for the study area were not available and thus calibrated by comparing the simulation results with the measured sediment samples at the Fisher station from 1992 to 1996. A comparison of the measured and simulated sediment load using the calibrated parameters (Table 2) resulted in an NSE equal to 0.59 (Fig. 3c and 3d). Note that during the calibration period, the RDP data were not available and thus the calibration values were determined based entirely on the gauge network. The calibrated parameters were then used for the simulation period (2013–2019), with the first two years used for the initialization of the model.

3.2. Point-pair comparisons of precipitation

To better understand the impacts of using radar rainfall as opposed to the gauged rainfall, a comparison between the daily precipitation at the Rantoul and Normal stations, and the radar in their nearest-neighboring grid cells was conducted. The two-point pairs were analyzed in terms of the annual precipitation total, monthly precipitation average, and rain-day frequency. For average annuals, radar precipitation was higher than the gauge precipitation but not significantly different based on the *t*-test

($p > 0.05$) (Table 3). This is also in line with the results for the average areal precipitation for the watershed where the areal radar-based rainfall was higher than the gauge-based rainfall (Fig. 1). In general, however, both sites showed similar patterns in terms of precipitation depth for yearly and monthly precipitation, and noticeable differences between the two datasets were not observed (Fig. 4). The radar at both sites showed higher rain-day frequencies for light precipitation and lower frequencies for heavy precipitation compared to the frequencies of gauge (Table 3). The underestimation of moderate and heavy precipitation frequency can be due in part to the attenuation of radar signal with heavy rainfall, range fade (i.e., beam overshoots the rainfall as the beam elevation above ground increases with increasing distance from the radar site) (Pathak and Teegavarapu, 2018), and the occurrence of smoothing when the data were gridded (Ensor and Robeson, 2008).

Despite the similarities in the two datasets, it was hypothesized that the traditional statistical descriptors (e.g. annual total and monthly average precipitation) may not have captured the differences in these

Table 2
Calibration parameters used in simulations.

Parameters	Value
Average hydraulic conductivity	0.4mm/hr
Mean fall velocity (w)	0.005 m/s
Erodibility of bed (M^*)	0.50g/m^2/s
Erosion exponent (b)	4
Critical shear stress (τ_{cd} and τ_{ce})	0.02N/m^2

Table 3
Point-pair comparisons of precipitation at Rantoul and Normal sites.

	At Rantoul site		At Normal site	
	Radar	Gauge	Radar	Gauge
Annual total [mm/year]	1,154	1,071	1,074	1,052
p-value	0.11		0.55	
Rain-day frequency for low rainfall	0.75 ± 0.027	0.63 ± 0.036	0.76 ± 0.026	0.67 ± 0.034
Rain-day frequency for moderate rainfall	0.21 ± 0.025	0.29 ± 0.035	0.20 ± 0.025	0.27 ± 0.032
Rain-day frequency for heavy rainfall	0.05 ± 0.013	0.08 ± 0.021	0.04 ± 0.011	0.06 ± 0.017

Note. The frequency values indicate the mean rain-day frequency with 95% confidence interval
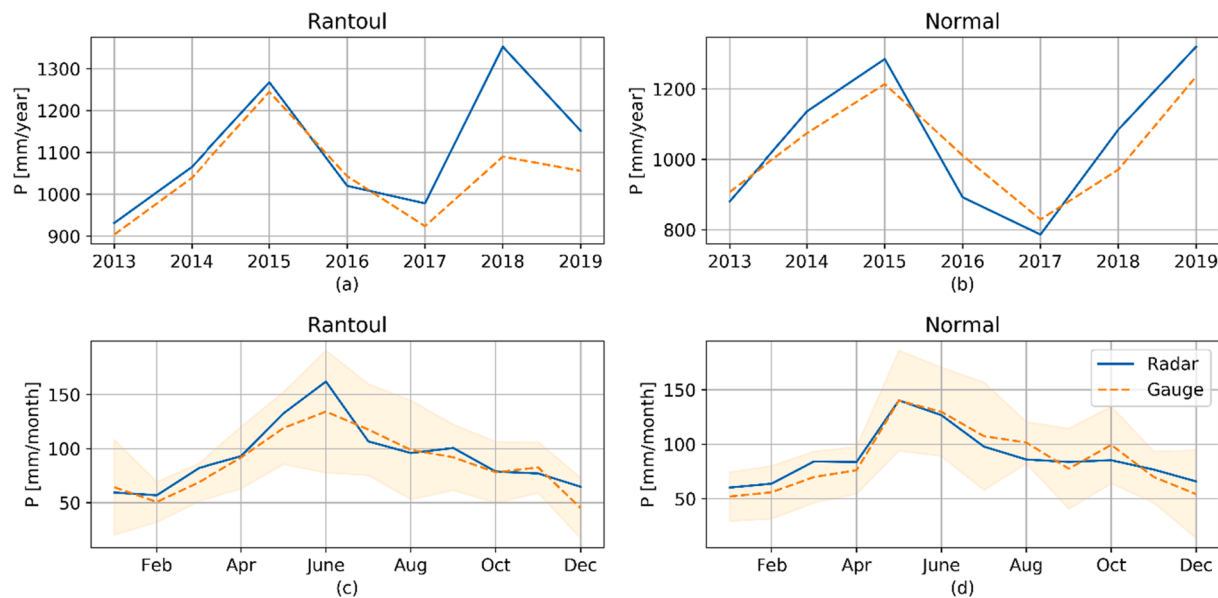
Fig. 4. Precipitation comparisons between radar and gauge products of annual average (a) at Rantoul and (b) at Normal sites, and monthly precipitation (c) at Rantoul and (d) at Normal sites with 95% confidence interval bands of gauge.

datasets since these descriptors cannot quantify the spatial variability of precipitation. The influences of the spatial distributions of rainfall estimates throughout the watershed were therefore evaluated in terms of their impacts on streamflow and sediment discharge.

3.3. Impacts of improved streamflow

To determine whether or not the improvement in sediment prediction was driven by the improvement in streamflow prediction due to the use of radar precipitation (hypothesis 1), sediment yield from 2015 to 2019 were quantified using three objective functions, the NSE, MAD, and RMSE (Table 4). In addition, monthly simulation results of areal mean precipitation across the watershed, streamflow, and sediment discharge at Fisher station for the entire simulation period are shown in Fig. 5. Note that precipitation and streamflow discharge are the same between the semi-distributed and distributed models so that only D-R and D-G results were included in Fig. 5a and 5b.

The simulation results indicated that using the radar improved the streamflow simulations compared to the observed streamflow discharge at Fisher station (Table 1 and Fig. 5b). However, it was proven that improved flow predictions did not necessarily improve the sediment yield predictions. The two models with radar inputs (D-R and S-R) indicated that even though the streamflow discharge prediction improved by radar, when semi-distributed sediment sources were provided, the reliable prediction for sediment yield cannot be guaranteed (S-R in Table 4). Therefore, the hypothesis that the improved streamflow would improve sediment transport and yield predictions did not hold in this case.

3.4. Impacts of spatial variations in precipitation

Hypothesis 2 is an alternative scenario for hypothesis 1 that the sediment predictions are still improved, without noticeable improvements observed in streamflow. To examine this hypothesis, two peaks observed in the simulation period were selected. There were remarkable differences for sediment yield between D-R and D-G at high peaks, such as in December 2015 and in October 2018 (Fig. 5c), even if streamflow differences in these periods were not noticeable (Fig. 5b). For these reasons, these two events estimated by D-R and D-G were further examined to evaluate hypothesis 2.

The heaviest rain events that occurred in December 2015, captured by radar and gauge are shown in Fig. 6. Based on both observations, we can infer that the heaviest rainfall was developed from the southeast of the watershed, where the Rantoul station was located, and moved to the northwest of the watershed (Fig. 6a-6c and Fig. 6d-6f). The radar showed the spatial variations of precipitation throughout the watershed. However, since rainfall estimates by the gauge networks were based entirely on the point observations, this created significant discrepancies between the two products. For instance, the rainfall estimates on the last day of the rain event reported zero value for the Rantoul station (Fig. 6f) while the radar showed some variations from 36 *mm* to 49 *mm* for the corresponding area (Fig. 6c). The underestimation of rainfall, especially on the last day of the event (Fig. 6c and 6f), resulted in the underestimation of sediment yield in December 2015. In other words, zero precipitation was reported at Rantoul station on the last day of the event, assigning zero precipitation for most of the watershed. This resulted in a misrepresentation of the highest peaks of sediment discharge during the simulation period when the gauge was used (Fig. 5c).

In contrast to the December 2015 event, the differences between the rainfall estimates between D-R and D-G across the watershed were not noticeable in October 2018 (Fig. 5a). Despite the fact that the amounts of streamflow were almost the same (Fig. 5b), the gauge produced a peak in sediment load in October 2018 that was not observed in the radar (Fig. 5c). To understand the discrepancies, the daily simulation results for the areal mean precipitation, total soil loss (sediment source), streamflow, and sediment yield at Fisher station were examined in detail (Fig. 7). The three largest peaks for soil loss estimations by gauge were observed on July 6, August 7, and September 7 in 2018 (Fig. 7b), and the peaks of rain events estimated by the gauge network yielded extreme peaks for sediment sources throughout the watershed. Even though
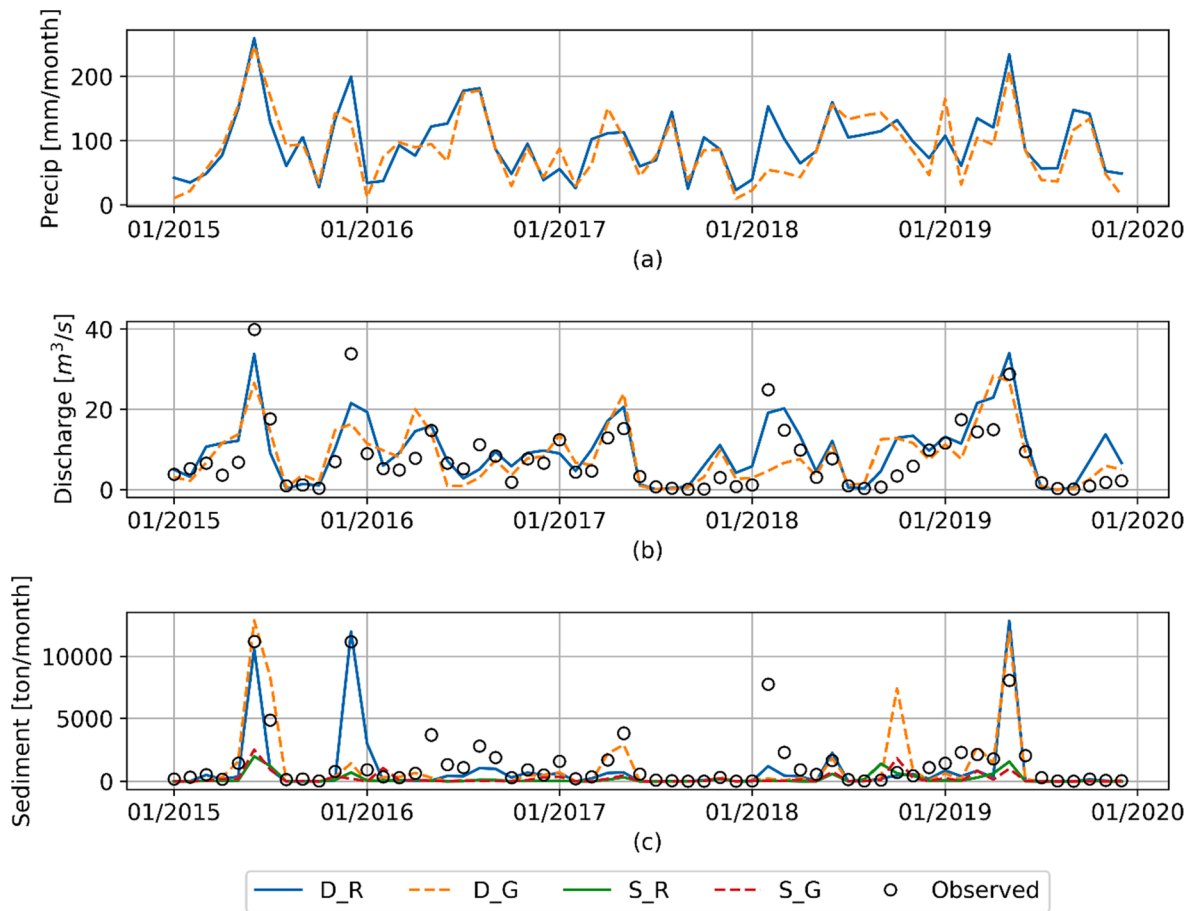
Table 4
Comparisons of model performance based on Nash-Sutcliffe Efficiency (NSE), Mean Absolute Difference (MAD), and Root-mean-square Error (RMSE).

	Streamflow [$m^3 s^{-1}$]		Sediment yield [ton day^{-1}]			
	Radar	Gauge	D-R	D-G	S-R	S-G
Mean	9.72	8.30	31.13	34.52	6.64	7.45
r^2	0.84	0.69	0.84	0.66	0.66	0.52
NSE	0.63	0.45	0.61	0.23	−0.09	−0.12
MAD	3.94	4.14	27.57	34.48	44.17	43.87
RMSE	5.01	6.11	49.78	70.05	83.32	84.16

Note. The NSE values were dimensionless.

Fig. 5. Simulation results of (a) monthly total areal average precipitation across the watershed (b) average streamflow discharge at Fisher station with 95% confidence interval bands of observed discharge and (c) monthly total sediment yield at Fisher station for the distributed model (D-R and D-G) and semi-distributed model (S-R and S-G).
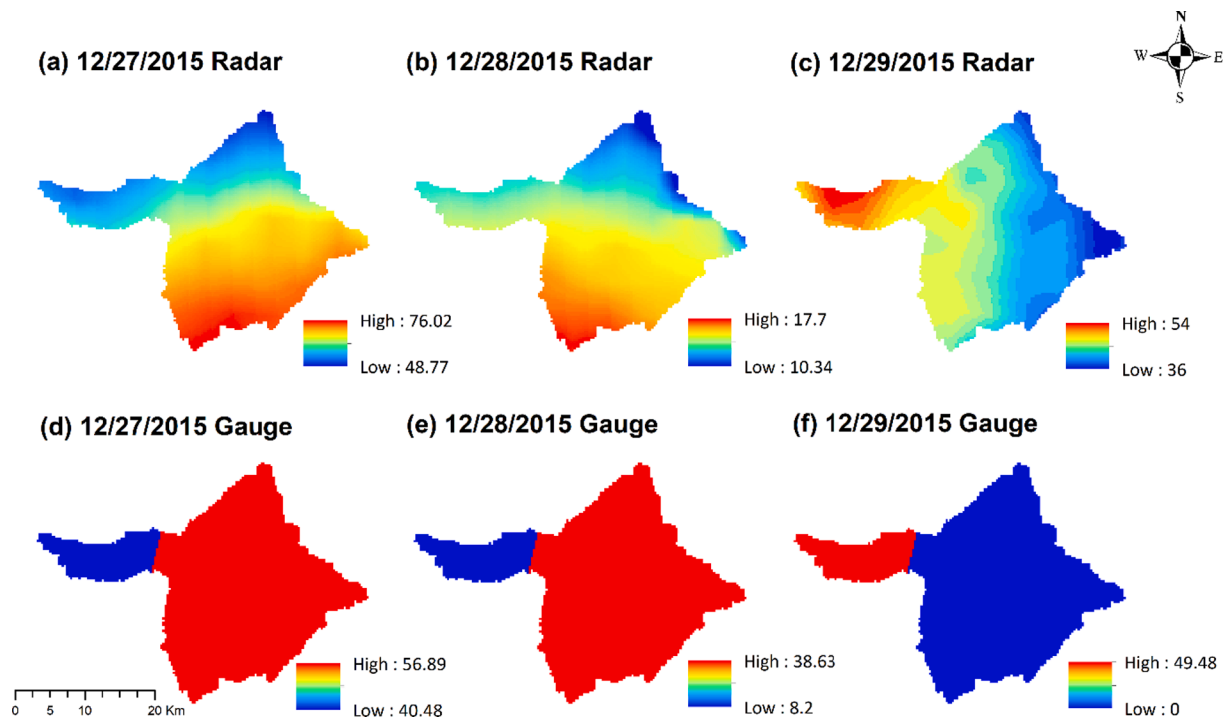

Fig. 6. The heaviest rainfall event in December 2015 captured by radar (top) and by gauge (bottom) across the watershed (units are in mm/day).
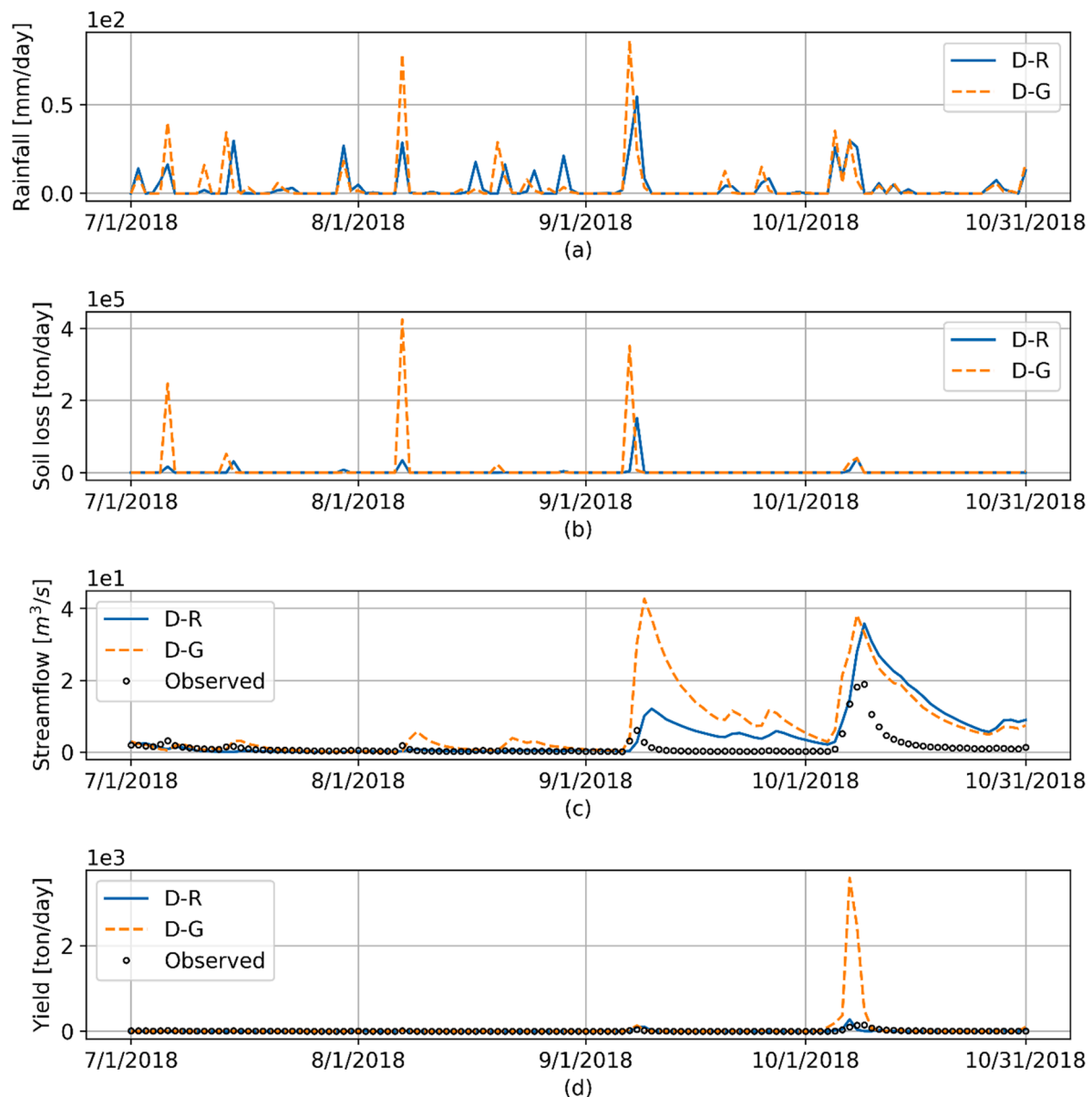
Fig. 7. Daily simulation results of (a) areal mean rainfall across the watershed, (b) total sediment production across the watershed, (c) streamflow discharge at Fisher station, and (d) sediment yield at Fisher station.

large amounts of sediment production were generated, the majority of sediment were deposited along their way because of the dry conditions (i.e. flow depth in overland flow and streamflow were too small to carry the suspended sediment) (Fig. 7c) and thus sediment yield at the Fisher station was relatively low compared to the peak in October (Fig. 7d). The peak of sediment yield in October occurred as the flowing water detached the deposited soil particles throughout the watershed and transported the soil particles downstream. In contrast to the flood peak that occurred in September, precipitation at the Normal site reported relatively heavy rain (54 *mm* on October 8, 2018). This rain event, along with the higher antecedent moisture conditions, detached and transported the deposited sediment for most parts of the watershed, resulting in the high peak of sediment yield at the outlet in October (Fig. 7d). From the simulation results, only a few peaks of rainfall estimated in the past can have a critical impact on predicting sediment discharge even several months later.

The total rainfall estimated for the entire watershed for the three dates that generated soil loss peaks in 2018 were 71 *mm* and 204 *mm*, for D-R and D-G, respectively (Fig. 8). The radar estimates reported extreme

rainfall rates only for the small portion of the watershed (i.e., clusters), and the rest of the watershed received relatively small amounts of rain for these three dates (Fig. 8a-8c), generating relatively small amounts of soil loss and streamflow compared to the D-G simulation. In terms of soil loss and streamflow discharge in October, both D-R and D-G simulations showed similar results since the precipitation rates were similar throughout the watershed (Fig. 7a-7c). However, the consequences of overestimating the rainfall in the past dates (Fig. 8d-8f) resulted in completely different estimations of sediment yield in October (Fig. 5d). Hence, based on the discrepancies investigated in the simulated sediment peaks in 2015 and 2018, misestimating a few heavy rainfall events can result in unreasonable predictions of sediment yield in both short- and long-term predictions. Therefore, we concluded that sediment transport process is driven by rainfall as threshold-like processes across the watershed, and thus resolving spatial variations in precipitation would improve sediment predictions at high peaks. In other words, we accepted hypothesis 2 that the use of RDP would improve sediment transport predictions regardless of streamflow predictions.
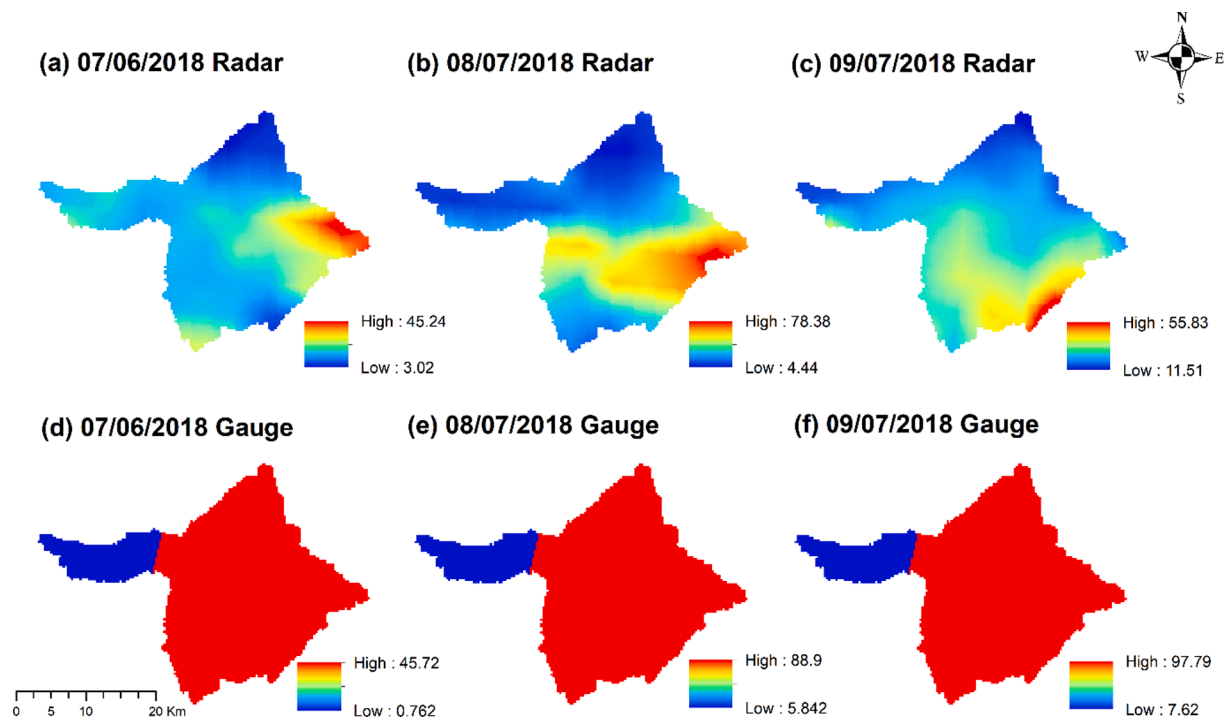
Fig. 8. Spatial distributions of rainfall estimates for the peaks of rain events occurred in 2018 captured by radar (top) and by gauge (bottom) across the watershed (units are in mm/day).

3.5. Impacts of semi- and distributed sediment sources

To evaluate hypothesis 3 that the use of RDP can improve the sediment predictions only when spatially distributed sediment sources are provided, the simulation results using the semi-distributed sediment source (S-R and S-G) were examined. Both results did not correspond with the observations well (Table 4) and failed to capture the high peaks in the simulation period (Fig. 5c) regardless of the precipitation inputs. Both S-R and S-G results showed the underestimation of sediment yield. By averaging the values of the input data such as slope and soil properties in the semi-distributed model (Fig. 9a), the contributions from the most vulnerable areas to soil erosion, where the rate of soil loss was significant, were not properly represented. These misrepresentations of the main forcing variables resulted in misestimating soil loss distribution across the watershed, failing to capture most of the peaks observed in distributed mode (Fig. 9b). Therefore, we accepted hypothesis 3 that the use of RDP would improve sediment predictions only where sediment sources are spatially distributed.

Based on the experiments for the three hypotheses using the four

models, we found that distributed precipitation such as RDP can improve sediment predictions only if sediment sources are spatially distributed. Sediment transport processes rely on co-located rainfall events and sediment sources. Therefore, modeling one without the other means that the combined effects of extreme precipitation and vulnerable areas are not conceptualized properly. Hence improved sediment predictions are only guaranteed when the spatial characteristics of both rainfall and sediment sources are addressed at a finer scale.

Overall, the simulation results indicated that the use of both finer resolution precipitation and soil loss could improve the representation of systemic responses of distributed hydrologic models for sediment discharge. If sediment production were estimated using semi-distributed models, the local input characteristics such as slope and soil properties may be lumped together, ignoring the contributions from the most vulnerable areas and this may cause the failure of capturing the high peaks or underestimation of sediment prediction (Fig. 9). Similarly, the most important advantage of radar-derived rainfall was its ability to capture the spatial variations of rainfall (i.e., pattern and intensity) across the watershed. This is especially crucial if rainfall events
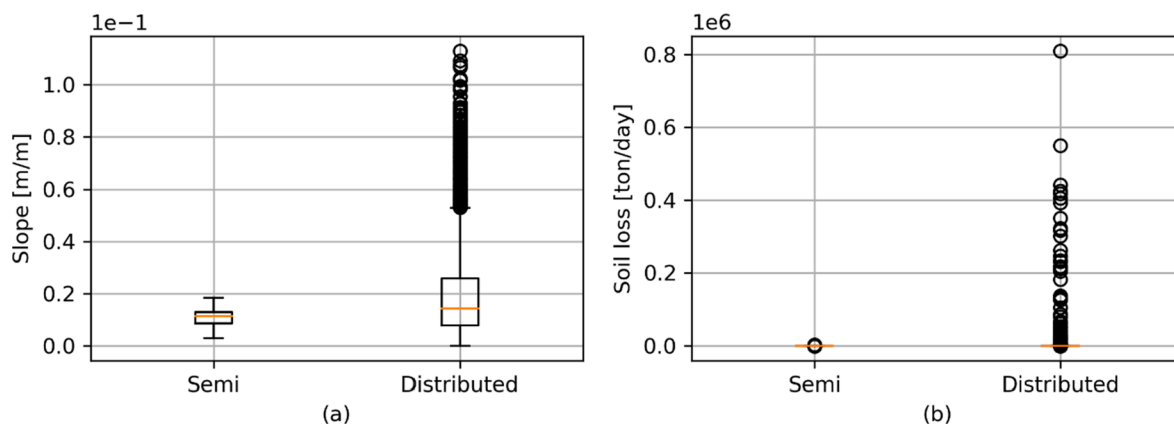

Fig. 9. (a) Assigned values of slope across the watershed, and (b) soil loss simulation results of the semi-distributed vs. distributed models.

characterized by the development of rainfall clusters across the watershed can result in significant localized sediment production and transport. The use of gauge networks may under- or over-estimate sediment loads as a function of the distance from the rainfall clusters even if the simulated streamflow is not significantly different from the radar simulation. This is expected to be exacerbated in agricultural fields, which are the major sediment source around the world, because of the unevenly distributed gauge stations, with a bias towards mountain valleys and populated areas (Ensor and Robeson, 2008; Liebmann and Allured, 2005).

This study has confirmed, that the full potential of using a radar-derived rainfall in predicting sediment production and delivery can only be achieved when using a distributed sediment transport model. Thus, the seamless integration of high-resolution input data to distributed hydrologic models can result in better predictive power, especially for the fate and transport phenomena, including sediment, where the spatio-temporal characteristics of precipitation and sediment production at finer resolution is essential.

4. Summary and conclusions

This study evaluated the impacts of using a semi-distributed and a distributed sediment source model with gauged- and radar-based precipitation on sediment predictions. An intensively managed agricultural watershed in central Illinois that typically represents the agricultural landscape across the Midwest was selected as a study area. The hillslope erosion model (WEPP) integrated with the physically-based hydrologic model MIKE SHE was used to estimate daily flow and sediment sources in either semi-distributed or fully distributed spatial discretization. Four models, rain-gauge-based and radar-rainfall-based models with two types of sediment sources were evaluated based on their capability to simulate streamflow, sediment production, and sediment transport. The multi-annual simulation results were compared to the observed discharge and daily sediment discharge estimated by the sediment rating curves. All of the three objective functions (NSE, MAD, and RMSE) indicated that the model prediction improved with the use of RDP in a distributed sediment source setting. The results with the semi-distributed sediment source showed significant disagreement with the observed data for sediment yield regardless of precipitation inputs. For the use of distributed sediment sources, the significant discrepancies of sediment discharge were observed at high peaks between the radar- and gauge-based simulations that were mainly due to the lack of spatial variability in the gauged precipitation. Considering the distances between the watershed and the gauged stations in this study, the gauge network failed to capture the occurrences of local precipitation events and thus could not account for sediment production and transport. The use of radar-derived rainfall, however, can eliminate this concern by improving the spatial discretization of precipitation across the watershed and hence, resulted in a better predictive power of the streamflow and sediment transport models.

The traditional methods such as Thiessen polygons for assigning precipitation based on gauge networks can result in a critical misrepresentation of precipitation variability, including missing data, and the irregular distribution of gauges with a bias towards the mountainous valley and densely populated areas. The lack of certain periods of data and spatial bias issues can lead to poor simulation results. In particular, since agricultural fields are major sources of sediment, bias and errors may even worsen for sediment prediction if the rain gauges were not densely installed. The use of Thiessen polygon with two gauge stations may be a worst-case scenario and thus if gauge-network is only available, other methods such as linear interpolation should be carefully considered to assign precipitation across the watershed to improve the model performance. In addition, evaluating soil loss at a larger scale can result in misrepresentation of spatial characteristics across the watershed, and thus the use of rain gauge network in lumped- or semi-distributed sediment models cannot represent actual field conditions

and the consequences of the spatial distribution of soil erosion.

The integration of the spatial characteristics of rainfall and soil loss at a finer scale is essential, particularly in simulating fate and transport phenomena that are directly driven by rain-drop impacts and flowing water. The findings in the present study indicated that enhancing distributed models by seamlessly integrating higher resolution precipitation and sediment production inputs is critical to advance the prediction of sediment transport and yield in both short- and long-term simulations. In this paper, daily time step and field-scale spatial resolution were used due to the model's limitations in managing large datasets. The use of finer resolution input data is expected to improve the model performance, and thus a tool that can seamlessly integrate these datasets should be developed. In contrast, the lumped or semi-distributed soil loss models can lead to unreliable simulation results as they can wipe out the vulnerable area to soil erosion, resulting in missing high peaks of sediment source across the watershed. In addition, the use of RDP may not significantly impact the hydrologic response of the system in terms of streamflow. However, in terms of the sediment predictions, the radar-rainfall-based simulation enhanced model performance only with the distributed sediment sources, while the gauge simulations failed to capture localized rain events that can significantly impact the fate and transport processes of sediment. In particular, the spatial misrepresentation of high intensity rainfall events resulted in the exacerbation of the discrepancies of sediment prediction compared to the streamflow prediction. This is due in part to sediment prediction being driven not only by precipitation but also by the subsequent convolution of the hydrologic and transport processes that can further enhance the uncertainties from precipitation. The use of RDP data with fully distributed settings in hydrologic and environmental models is expected to improve the predictions of systemic responses resulting in a better understanding of transport processes that are crucial for the implementation of conservation and mitigation practices.

CRediT authorship contribution statement

Sanghyun Lee: Conceptualization, Methodology, Software, Data curation, Formal analysis, Investigation, Writing - original draft, Writing - review & editing. **Maria L. Chu:** Conceptualization, Writing - review & editing, Validation, Supervision, Project administration, Funding acquisition. **Jorge A. Guzman:** Software, Validation, Supervision.

Declaration of Competing Interest

The authors declare that they have no known competing financial interests or personal relationships that could have appeared to influence the work reported in this paper.

References

Arnone, E., Pumo, D., Viloa, F., Noto, L.V., Loggia, G., 2013. Rainfall statistics changes in Sicily. Hydrol. Earth Syst. Sci. 17, 2449–2458. https://doi.org/10.5194/hess-17-2449-2013.

Azadi, S., Nozari, H., Godarzi, E., 2020. Predicting sediment load using stochastic model and rating curves in a hydrological station. J. Hydrol. Eng. 25, 05020017. https://doi.org/10.1061/(ASCE)HE.1943-5584.0001967.

Botero-Acosta, A., Chu, M.L., Huang, C., 2019. Impacts of environmental stressors on nonpoint source pollution in intensively managed hydrologic systems. J. Hydrol. 579, 124056 https://doi.org/10.1016/j.jhydrol.2019.124056.

Chaplot, V., Saleh, A., Jaynes, D.B., 2005. Effect of the accuracy of spatial rainfall information on the modeling of water, sediment, and NO_3–N loads at the watershed level. J. Hydrol. 312, 223–234. https://doi.org/10.1016/j.jhydrol.2005.02.019.

Di Luzio, M., Arnold, J.G., 2004. Formulation of a hybrid calibration approach for a physically based distributed model with NEXRAD data input. J. Hydrol. 298, 136–154. https://doi.org/10.1016/j.jhydrol.2004.03.034.

Ensor, L.A., Robeson, S.M., 2008. Statistical characteristics of daily precipitation : comparisons of gridded and point datasets. J. Appl. Meteorol. Climatol. 47, 2468–2476. https://doi.org/10.1175/2008JAMC1757.1.

Fischer, F.K., Kistler, M., Brandhuber, R., Maier, H., Treisch, M., Auerswald, K., 2018. Validation of official erosion modelling based on high-resolution radar rain data by aerial photo erosion classification. Earth Surf. Process. Landforms 43, 187–194. https://doi.org/10.1002/esp.4216.

Flanagan, D., Nearing, M., 1995. USDA-Water Erosion Prediction Project (WEPP) hillslope profile and watershed model documentation, NSERL REPORT #10. USDA-ARS National Soil Erosion Research Laboratory, West Lafayette, IN.

Gao, J., Sheshukov, A.Y., Yen, H., White, M.J., 2017. Impacts of alternative climate information on hydrologic processes with SWAT: A comparison of NCDC, PRISM and NEXRAD datasets. Catena 156, 353–364. https://doi.org/10.1016/j.catena.2017.04.010.

Gelder, B., Sklenar, T., James, D., Herzmann, D., Cruse, R., Gesch, K., Laflen, J., 2018. The Daily Erosion Project – daily estimates of water runoff, soil detachment, and erosion. Earth Surf. Process. Landforms 43, 1105–1117. https://doi.org/10.1002/esp.4286.

IDOA, 2018. Illinois soil conservation transect survey summary report [WWW Document]. URL https://www2.illinois.gov/sites/agr/Resources/LandWater/Pages/Illinois-Soil-Conservation-Transect-Survey-Reports.aspx (accessed 8.13.18).

IEPA, 2007. Sangamon River/Lake Decatur watershed TMDL report. Springfield, IL.

Kalin, L., Hantush, M.M., 2006. Hydrologic modeling of an eastern Pennsylvania watershed with NEXRAD and rain gauge data. J. Hydrol. Eng. 11, 555–569. https://doi.org/10.1061/(ASCE)1084-0699(2006)11.

Krajewski, W.F., Vignal, B., 2001. Evaluation of anomalous propagation echo detection in WSR-88D data: A large sample case study. J. Atmos. Ocean. Technol. 18, 807–814. https://doi.org/10.1175/1520-0426(2001)018<0807:EOAPED>2.0.CO;2.

Kristensen, K.J., Jensen, S.E., 1975. A model for estimating actual evapotranspiration from potential evapotranspiration. Hydrol. Res. 6, 170–188. https://doi.org/10.2166/nh.1975.0012.

Laflen, J.M., Flanagan, D.C., Engel, B.A., 2004. Soil erosion and sediment yield prediction accuracy using WEPP. J. Am. Water Resour. Assoc. 40, 289–297. https://doi.org/10.1111/j.1752-1688.2004.tb01029.x.

Lee, S., Chu, M.L., Guzman, J.A., Botero-Acosta, A., In press. A comprehensive modeling framework to evaluate soil erosion by water and tillage. J. Environ. Manage. 111631. https://doi.org/10.1016/j.jenvman.2020.111631.

Liebmann, B., Allured, D., 2005. Daily precipitation grids for South America. Bull. Am. Meteorol. Soc. 86, 1567–1570. https://doi.org/10.1175/BAMS-86-11-1567.

Lin, Y., 2011. GCIP/EOP surface: precipitation NCEP/EMC 4KM gridded data (GRIB) stage IV data. version 1.0. UCAR/NCAR - Earth Observing Laboratory [WWW Document]. URL https://doi.org/10.5065/D6PG1QDD (accessed 6.16.20).

Nash, J.E., Sutcliffe, J.V., 1970. River flow forecasting through conceptual models part I - A discussion of principles. J. Hydrol. 10, 282–290. https://doi.org/10.1016/0022-1694(70)90255-6.

Nelson, B.R., Seo, D.J., Kim, D., 2010. Multisensor precipitation reanalysis. J. Hydrometeorol. 11, 666–682. https://doi.org/10.1175/2010JHM1210.1.

Orlanski, I., 1975. A rational subdivision of scales for atmospheric processes. Bull. Am. Meteorol. Soc. 56, 527–530.

Pathak, C.S., Teegavarapu, R.S.V., 2018. Radar rainfall data estimation and use. American Society of Civil Engineers, Reston, Virginia.

Refsgaard, J.C., Storm, B., 1995. MIKE SHE. In: Singh, V.P. (Ed.), Computer Models of Watershed Hydrology. Water Resources Publications, Colorado, pp. 809–846.

Rhoads, B.L., Lewis, Q.W., Andresen, W., 2016. Historical changes in channel network extent and channel planform in an intensively managed landscape: Natural versus human-induced effects. Geomorphology 252, 17–31. https://doi.org/10.1016/j.geomorph.2015.04.021.

Smith, J.A., Seo, D., Baeck, M.L., Hudlow, M.D., 1996. An intercomparison study of NEXRAD precipitation estimates. Water Resour. Res. 32, 2035–2045. https://doi.org/10.1029/96WR00270.

Syvitski, J.P., Morehead, M.D., Bahr, D.B., Mulder, T., 2000. Estimating fluvial sediment transport: The rating parameters. Water Resour. Res. 36, 2747–2760. https://doi.org/10.1039/C7RE00129K.

Tfwala, S.S., Wang, Y.M., 2016. Estimating sediment discharge using sediment rating curves and artificial neural networks in the Shiwen River. Taiwan. Water (Switzerland) 8, 53. https://doi.org/10.3390/w8020053.

Tiwari, A.K., Risse, L.M., Nearing, M.A., 2000. Evaluation of WEPP and its comparison with USLE and RUSLE. Trans. Am. Soc. Agric. Eng. 43, 1129–1135. https://doi.org/10.13031/2013.3005.

Urban, M.A., Rhoads, B.L., 2003. Catastrophic human-induced change in stream-channel planform and geometry in an agricultural Watershed, Illinois. USA. Ann. Assoc. Am. Geogr. 93, 783–796. https://doi.org/10.1111/j.1467-8306.2003.09304001.x.

USDA, 2017. Web soil survey [WWW Document]. United States Dep. Agric. URL https://www.nrcs.usda.gov/wps/portal/nrcs/main/soils/survey/ (accessed 4.14.18).

USDA, 2016. USDA-NASS Cropland Data Layer [WWW Document]. United States Dep. Agric. URL https://nassgeodata.gmu.edu/CropScape/ (accessed 3.12.17).

USGS, 2016. National Elevation Dataset (NED) [WWW Document]. United States Dep. Agric. URL https://earthexplorer.usgs.gov/ (accessed 3.12.17).

Usón, A., Ramos, M.C., 2001. An improved rainfall erosivity index obtained from experimental interrill soil losses in soils with a mediterranean climate. Catena 43, 293–305. https://doi.org/10.1016/S0341-8162(00)00150-8.

Vasiloff, S.V., Seo, D.J., Howard, K.W., Zhang, J., Kitzmiller, D.H., Mullusky, M.G., Krajewski, W.F., Brandes, E.A., Rabin, R.M., Berkowitz, D.S., Brooks, H.E., McGinley, J.A., Kuligowski, R.J., Brown, B.G., 2007. Improving QPE and very short term QPF: An initiative for a community-wide integrated approach. Bull. Am. Meteorol. Soc. 88 (12), 1899–1911. https://doi.org/10.1175/BAMS-88-12-1899.

Wei, W., Chen, L., Fu, B., 2009. Effects of rainfall change on water erosion processes in terrestrial ecosystems : a review. Prog. Phys. Geogr. 33, 307–318. https://doi.org/10.1177/0309133309341426.

Wischmeier, W.H., Smith, D.D., 1978. Predicting rainfall erosion losses: a guide to conservation planning, U.S. Department of Agriculture Handbook No. 537. https://doi.org/10.1029/TR039i002p00285.

Zhang, X.C., Nearing, M.A., Risse, L.M., McGregor, K.C., 1996. Evaluation of WEPP runoff and soil loss predictions using natural runoff plot data. Trans. Am. Soc. Agric. Eng. 39, 855–863. https://doi.org/10.13031/2013.27570.